14q32 Noncoding RNAs in vascular remodelling

Goossens, E.A.C.

Chapter 6

Inhibition of Cold-Inducible RNA-Binding Protein decreases 14q32 microRNA miR-495 expression and enhances *in vitro* angiogenesis

Manuscript in preparation

EAC Goossens[1,2]
L Zhang[1,2]
PHA Quax[1,2]
AY Nossent[1,3,4]

[1]Department of Surgery and [2]Einthoven Laboratory for Experimental Vascular Medicine, Leiden University Medical Center, Leiden, The Netherlands; [3]Department of Internal Medicine II and [4]Department of Laboratory Medicine, Medical University of Vienna, Vienna, Austria

Abstract

Aims: In peripheral artery disease (PAD) an occluded artery leads to downstream tissue ischemia. To restore blood flow, angiogenesis, an ischemia-driven neovascularization process, is needed. Inhibition of 14q32 microRNAs miR-495-3p and miR-329-3p improves post-ischemic neovascularization. Using SILAC followed by pre-microRNA pulldown and Mass Spectrometry, Cold-inducible RNA-binding protein (CIRBP) was found to regulate these microRNAs. CIRBP expression is induced by hypothermic stress, an important component of PAD. Therefore, we hypothesized that CIRBP inhibition can improve post-ischemic angiogenesis via inhibition of 14q32 microRNA expression.

Methods and results: In this study, we investigated the regulatory mechanisms of CIRBP in relation to 14q32 microRNA expression and angiogenesis *in vitro*. We assessed expression of different CIRBP splice variants (CIRBP-SVs), as well as antisense lncRNA CIRBP-AS1 in hypothermia. We used siRNAs to determine how CIRBP and CIRBP-AS1 regulate each other, 14q32 microRNA expression and angiogenesis. In HUVECs cultured at 32°C for 24h and 48h, CIRBP expression was upregulated, but miR-495-3p and miR-329-3p expression remained unaffected. CIRBP-SV1 and miR-495-3p, but not miR-329-3p or CIRBP-SV2-4, were downregulated in HUVECs after CIRBP knockdown. To assess angiogenesis, scratch-wound healing assays and tube formation assays were performed and both improved migration and tube formation were observed after either CIRBP or CIRBP-AS1 knockdown. CIRBP-AS1 expression increased under hypothermia and decreased after CIRBP knockdown, mimicking the CIRBP-SV1 expression pattern. Similarly, knockdown of CIRBP-AS1, resulted in decreased expression of CIRBP, in particular of CIRBP-SV1, as well as inhibition of miR-329-3p and miR-495-3p expression.

Conclusions: Both CIRBP-SV1 and CIRBP-AS1 were upregulated under hypothermia without affecting miR-495-3p and miR-329-3p expression. However, total CIRBP and CIRBP-SV1 knockdown inhibited miR-495-3p expression and improved *in vitro* angiogenesis. Therefore, we conclude that CIRBP contributes to processing of miR-495-3p, but is not rate-limiting under normothermic conditions. CIRBP-SV1 and CIRBP-AS1 expression patterns closely mimicked each other under all experimental conditions. CIRBP-AS1 knockdown also increased angiogenesis and downregulated both miR-495-3p and miR329-3p. The mechanism of interaction will be studied *in vitro* and *in vivo*. Further exploration of CIRBP's function in post-ischemic neovascularization will be investigated in an *in vivo* hindlimb ischemia model, using $CIRBP^{-/-}$ mice.

Introduction

Peripheral artery disease (PAD) is caused by occlusions of the arterial vasculature in the lower limb, mainly the femoral artery, resulting in deprivation of blood flow, and thus of oxygen and nutrients, to the lower extremities. This shortage in blood supply leads to clinical features of painful and cold extremities (poikilothermia, i.e. inability to maintain core temperature). Other clinical features are pulselessness, pallor, paresthesia, paralysis. Together these symptoms are called the six Ps. Current treatment options include angioplasty procedures with stent placement and bypass surgery. However, these therapies have the risk of restenosis or bypass stenosis, and often they cannot be applied at all, because of anatomical restrictions or advanced stages of the disease. That is why other therapeutic neovascularization approaches are still required. The body has its own mechanism to restore blood flow to ischemic and cold tissues, namely neovascularization, the collective term for angiogenesis and arteriogenesis. In patients with severe PAD, this is insufficient to completely recover blood flow to the leg. Therefore, enhancing neovascularization is an interesting and promising new treatment option for patients with PAD. In this study we explored the role of the Cold-Inducible RNA Binding Protein (CIRBP) as a pro-angiogenic factor and study the potential of modulating CIRBP in order to enhance neovascularization. CIRBP is regulated by differential stress factors including ischemia[1, 2] and, as its name suggests, temperature[1, 3-6]. In fact, CIRBP was described in 1997 as the first cold shock protein that was induced at mild hypothermia[7] and this effect was conserved between humans and mice[8].

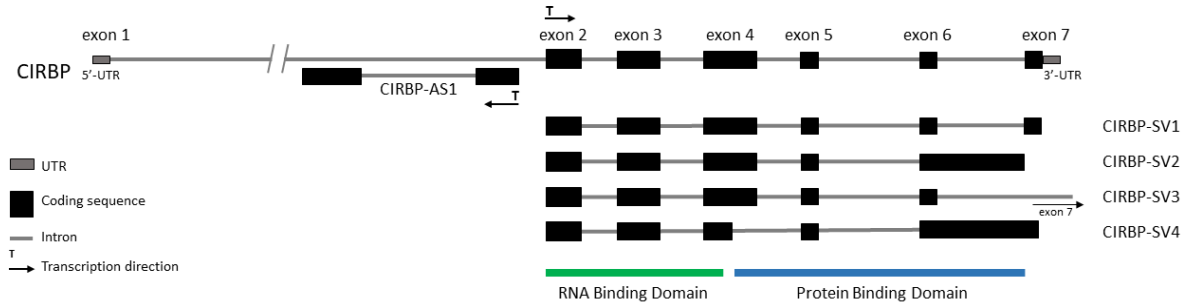

Figure 1 Schematic overview of CIRBP gene with splice variants and CIRBP-AS1. according to UCSC Genome Browser alignment GRCh38/hg38. Only splice variants affecting the protein coding sequence are depicted, however more variants are known that affect 5'- or 3'-UTR composition.

CIRBP is an RNA-binding protein (RBP) that influences post-transcriptional processing of its target RNA[9] and its gene is located at chromosome 19 in humans (Figure 1). CIRBP contains an N-terminal RNA-binding domain and a C-terminal domain that has protein binding properties[7, 10]. There are various splice variants of CIRPB which, in mice, showed altered expression patterns in response to hypothermia[11]. The four main splice variants in humans, CIRBP-SV1, CIRBP-SV2, CIRBP-SV3 and CIRBP-SV4, have the RNA-binding domain in common,

but have different C-termini. Furthermore, the antisense strand of CIRBP contains an antisense long noncoding RNA (CIRBP-AS1). Antisense long noncoding RNAs (lncRNAs) can have several functions. Antisense lncRNAs have been shown to affect transcription and support function of their respective coding sense-strand[12]. For example, lncRNA MALAT1 has an antisense transcript TALAM1 and together they function as a sense-antisense pair[13, 14]. Therefore, it is possible that either sense and antisense strands are co-transcribed and counteract or cooperate in their actions[12] or that one strand affects expression of the other strand.

CIRBP, as an RBP, does not only affect processing of messenger RNAs (mRNAs), but also has the ability to act in microRNA processing. MicroRNAs (miRs) are small noncoding RNA molecules of approximately 22 nucleotides in length. They are transcribed from DNA by RNA polymerase II into primary microRNAs. Next, these primary microRNAs (pri-miRs) are processed by Drosha, a processing complex, into precursor microRNAs (pre-miRs), which in turn are cleaved into two mature microRNA strands by the enzyme Dicer[15, 16]. Mature microRNAs are loaded into an RNA Induced Silencing Complex (RISC), which binds to the 3'-untranslated region of target mRNAs, leading to translational repression. Therefore, microRNAs are negative regulators of protein expression. Because a single microRNA has the ability to bind to a large number of target mRNAs, microRNAs can affect complete physiological and pathophysiological processes. However, the expression of microRNAs themselves can also be regulated, either transcriptionally or post-transctiptionally[17-19].

Previously, we showed that a large microRNA cluster located on chromosome 14 (14q32 locus), plays a regulatory role in different types of vascular remodelling, including atherosclerosis and restenosis, but also in post-ischemic neovascularization[20-23]. This cluster is also known as DLK1-DIO3 cluster and is conserved in mice where it is located at the 12F1 locus. CIRBP was shown to directly bind two precursors of 14q32 microRNAs, namely pre-miR-329 and pre-miR-495[18], thereby inducing the processing into the mature microRNAs miR-329-3p and miR-495-3p. In previous studies, we found that inhibition of 14q32 microRNAs miR-495-3p and miR-329-3p increased post-ischemic neovascularization[20]. At the same time, inhibition of these microRNAs also reduced post-interventional restenosis[21], potentially offering a double advantage for patients with severe PAD. Therefore, we hypothesized that inhibition of CIRBP leads to a decrease in mature miR-495-3p and miR-329-3p and consequently promotes post-ischemic neovascularization.

In this study, we first studied how hypothermic stress affects total CIRBP, its splice variants and its antisense lncRNA, and subsequently, 14q32 microRNA expression. Furthermore, we studied the effect of CIRBP and CIRBP-AS1 inhibition on angiogenesis.

Materials and Methods

Isolation of human umbilical cord arterial fibroblasts (HUAFibs), arterial smooth muscle cells (HUASMCs), venous endothelial cells (HUVECs) and arterial endothelial cells (HUAECs)

Primary human vascular cells were isolated as described earlier by Welten et al[20]. In brief, for HUAFib and HUASMC isolation, the arteries were removed and cleaned from remaining connective tissue. Endothelial cells were removed by gently rolling the artery over a blunted needle. The tunica adventitia and tunica media were separated using surgical forceps. After overnight incubation in HUAFib/HUASMC culture medium, (DMEM GlutaMAX™ (Invitrogen, GIBCO)), 10% heat inactivated fetal calf serum (FCSi) (PAA), 10% heat inactivated human serum, 1% penicillin (10000U/mL) / streptomycin (10000U/mL) and 1% nonessential amino acids (ref 11140-035, GIBCO, Life Technologies), the tunica adventitia and the tunica media separately were cut with scissors in pieces of maximum of 2mm incubated in a 2mg/ml collagenase type II solution (Worthington) at 37°C. Cell suspensions were filtered over a 70µm cell strainer and centrifuged at 400g for 10 minutes. Cell pellet was resuspended and plated in culture medium. Cells isolated from the tunica adventitia were washed with culture medium after 90 minutes to remove slow-adhering non-fibroblast cells. Cells isolated from tunica media were plated in 1% gelatin coated plates with culture medium.

For HUVEC and HUAEC isolation, respectively, the vein and the arteries were inserted with a cannula and was flushed with sterile PBS. The vessel was infused with 0.075% collagenase type II (Worthington) and incubated at 37°C for 20 minutes. The collagenase solution was collected and the vessel was flushed with PBS in order to collect all detached endothelial cells. The cell suspension was centrifuged at 400g for 5 minutes and the pellet was resuspended in HUVEC culture medium (EBM-2 (LONZA) with 2% FBS) HUVECs were cultured in plates coated with fibronectin from bovine plasma (Sigma).

Primary cell culture

HUAFibs and HUASMCs were cultured at 37°C in a humidified 5% CO_2 environment. Culture medium (DMEM GlutaMAX™ (Invitrogen, GIBCO)), 10% FCSi (PAA), 1% penicillin (10.000U/mL) / streptomycin (10.000U/mL)) was refreshed every 2-3 days. Cells were passed using trypsin (Sigma) at 70-80% confluency. HUAFibs were used for scratch-wound healing assay at passage four, HUVECS at passage three. Stock solutions of isolated HUAFibs up to

passage four and murine fibroblasts up to passage five were stored at -180°C in 50% DMEM GlutaMAX™ containing 10% FCSi and 1% Penicillin/Streptomycin, 40% FCSi (PAA) and 10% DMSO (Sigma). HUVECs were stored up to passage three in 90% heat-inactivated New Born Calf Serum (NBSCi) (Sigma) and 10% DMSO (Sigma).

Hypothermic HUVEC cell culture

Primary HUVECs were seeded in 12-well plates coated with fibronectin at 100.000 cells per well in culture medium. After overnight incubation at 37°C, cells were washed with PBS and new medium was applied before putting the plates in the right incubator: normothermic incubator 37°C and hypothermic incubator 32°C, all humidified and 5% CO_2 and 20% O_2. After 24 or 48 hours, cells were washed with PBS and 0.5mL TRIzol/well was added for RNA isolation. Each single condition was performed in triplicate and the hypothermia experiment was performed three independent times.

In vitro CIRBP and CIRBP-AS1 knockdown with siRNA transfection

Primary HUAFIBs were seeded in 12-well plates at 80.000 cells per well in culture medium, for HUVECs 100.000 cells per well. After 24 hours, cells were washed with PBS and each well was incubated with 900µL of Opti-MEM medium with 10% NBSCi for HUVECs and 1% penicillin/streptomycin for both cell types and, after 10 minutes of incubation of transfection medium, 100µL of transfection medium (94µL Opti-MEM with 3µL of Lipofectamine RNAiMax (Life Technologies) and 3µL of siRNA) was added. siRNA concentration used per well was 30nM. siRNAs used were siRNA CIRBP (sasi-172352), siRNA CIRPB-AS1 (sasi-208901) and siRNA NegCtrl: Mission universal Negative Control #1 (all Sigma-Aldrich). After addition of transfection agents, cells were put in the incubator at 37°C for 24 hours.

Migration assay - scratch-wound healing

After incubation of 24 hours, medium was aspired and a scratch-wound was made across the diameter of each well using a p200 pipet tip. Next, cells were washed with PBS and fresh starve medium (EBM-2 (LONZA) containing only 0.2% of FBS and 1% Gentamicin Amphotericin of the provided bulletkit) was added. In order to monitor scratch-wound closure, live phasecontrast microscropy (Axiovert 40C, Carl Zeiss) was used for taking pictures immediately after (0h) and 18 hours (HUVECs) after introducing the scratch-wound. Pictures were taken at two different locations in each well and averaged for analysis. Scratch size was calculated at 0h and 18h using the wound healing tool macro for ImageJ. Finally, cells were washed with PBS and 0.5mL TRIzol/well was added for RNA isolation. Each single scratch assay condition

was performed in triplicate and this scratch-wound healing assay was performed three independent times.

Tube formation assay

Tube formation assay was performed using HUVECs at passage three. At confluency, cells were transfected as described previously with Lipofectamine RNAiMax and siRNA CIRPB or siRNA Negative Control. After 24 hours, cells were counted and seeded on solidified Geltrex™ (ref: A14132-02, Gibco) in a 96-wells plate. Photos were taken using live phasecontrast microscropy at 12 hours after seeding and quantified using ImageJ Angiogenesis Analyzer. Each single tube formation assay was performed in 6 wells per condition and the independent tube formation assay was performed five independent times.

RNA isolation

RNA isolation of cultured cells was performed by standard TRIzol-chloroform extraction, according to the manufacturer's instructions (Thermo Fisher Scientific). RNA concentrations were measured using Nanodrop™ 1000 Spectrophotometer (Thermo Fisher Scientific).

MicroRNA Quantification

For microRNA quantification of miR-329-3p and miR-495-3p, in all samples RNA was reversed transcribed using the Taqman™ MicroRNA Reverse Transcription Kit (Thermo Fisher Scientific) and subsequently quantified using microRNA-specific Taqman™ qPCR kits (Thermo Fisher Scientific) on the VIIa7 (Thermo Fisher Scientific). MicroRNA expression was normalized against U6 small nuclear RNA.

mRNA, pri-microRNA and pre-microRNA quantification

For mRNA quantification of CIRBP, antisense lncRNA, primary microRNAs and precursor microRNAs, RNA was reverse transcribed using 'high-capacity RNA to cDNA kit' (Thermo Fisher Scientific) and quantified by qPCR using SybrGreen reagents (Qiagen) on the VIIa7. mRNA and antisense lncRNA expression was normalized against GAPDH and primary-microRNA and pre-microRNA expression was normalized to U6. Primer sequences are provided in Supplementary Table 1.

Statistical Analysis

Data are presented as mean ± SEM. Indicated differences have the following levels of significance: *p<0.05, **p<0.01, ***p<0.001, ****p<0.0001. All tests were performed with a significance level of α<0.05.

One-sample t-tests were performed to test differences of treated groups that are expressed relative to the negative control treatment, which is set to 100%. This test was used in knockdown experiments, hypothermia experiment and functional assays.

Differences in scratch wound healing van PCNA expression between CIRBP-AS1 siRNA and negative control siRNA treated cells were assessed using independent sample Student's t-tests.

One-way ANOVA test was performed to detect statistical significant differences over multiple groups. Between specific groups, the presence of differences was assessed with independent sample Student's t-tests, corrected for multiple testing. These tests were used in comparison of CIRBP expression in different vascular wall cell layers.

Results

CIRBP expression of in primary vascular cells

First, we determined total CIRBP gene expression in primary vascular cells originating from human umbilical cords. These cells were HUVECs, HUAECs, HUASMCs and HUAFIBs. CIRBP was expressed in cells derived from all layers of the vessel wall and no differences in expression levels were observed (Figure 2). However, as venous or capillary endothelial cells initiate angiogenesis and are thus leading cells in angiogenesis[24], we focused on HUVECs in all further experiments to study the pro-angiogenic potential of targeting CIRBP.

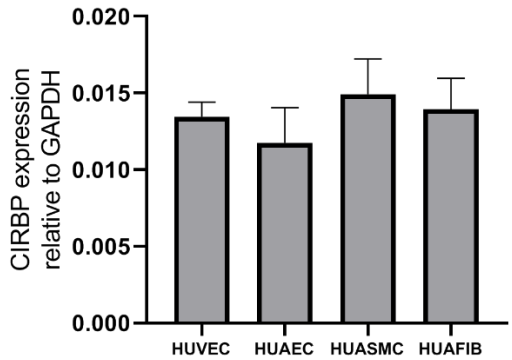

Figure 2 CIRPB expression in primary cells of human umbilical cord cell layers. For each cell type, total CIRBP mRNA expression was measured in three independent samples and did not show differences in expression between different vascular cell layers. Mean expression is indicated and error bars represent SEM. No significant differences were observed with one-way ANOVA (α<0.05).

Total CIRBP and CIRBP splice variants in hypothermia

Previous studies showed upregulated CIRBP expression under cellular stress conditions, including mild hypothermia[3]. Therefore, we measured total CIRBP expression in HUVECs that were subjected to mild hypothermia (32°C) either for 24 or 48 hours. Total CIRBP expression was increased after both 24 and 48 hours compared to the normothermic condition (37°C) with ~200% and ~70%, respectively (Figure 3B+C).

Furthermore, we measured the expression of four different splice variants (SV) of CIRBP shown in Figure 3A. Although not significant, CIRBP-SV1 expression was increased by ~80% at 24 hours (p=0.12) and by ~60% at 48 hours (p=0.14) of hypothermia (Figure 3D+E). The remaining three splice variants were not altered consistently over time under hypothermia, however.

CIRBP-AS1 in hypothermia

As CIRPB expression was induced in HUVECs under hypothermic conditions, we asked what would happen to the expression of the antisense long noncoding RNA of CIRBP (CIRBP-AS1) under hypothermia. CIRBP-AS1, like CIRBP, showed a trend towards increased expression of ~160% under hypothermia after 24 hours (p=0.096, Figure 4A) and we observed even further upregulated expression of ~220% after 48 hours of hypothermia (p=0.097, Figure 4B) compared to normothermia.

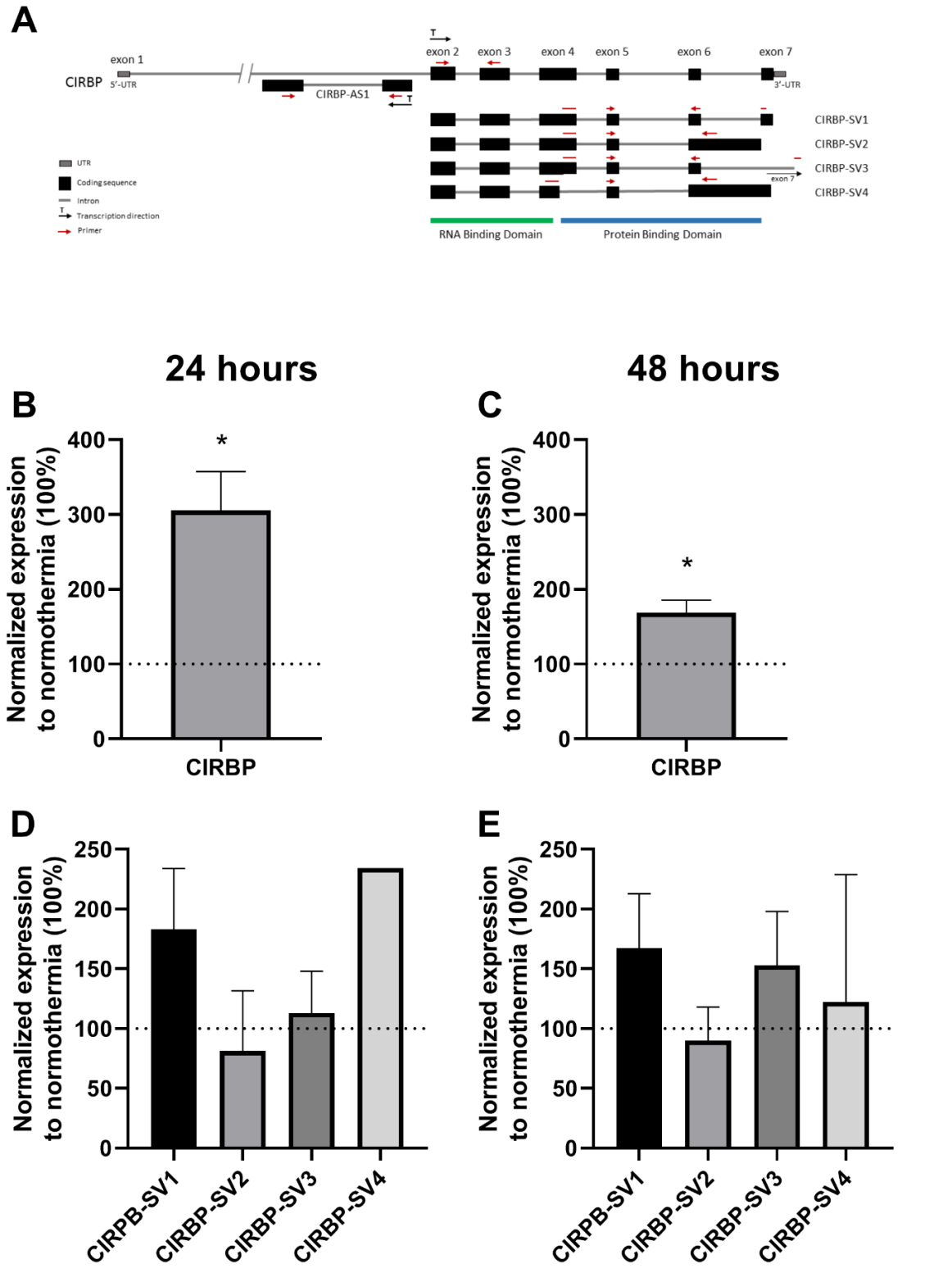

Figure 3A-E Total CIRBP and CIRBP splice variants expression after 24 or 48 hours hypothermia. A – schematic representation of the CIRBP gene and its splice variants with primer binding sites indicated. B+C – total CIRBP expression after 24 and 48 hours of hypothermia was induced compared to normothermic condition (200% increase and 70% increase, respectively). D+E – expression of CIRBP splice variants after 24 and 48 hours of hypothermia, respectively, was not changed significantly for any splice variant. Mean expression relative to GAPDH and normalized to normothermic condition (dotted line). Error bars represent SEM (N=3). One sample t-test is performed with $\alpha < 0.05$. *$p<0.05$.

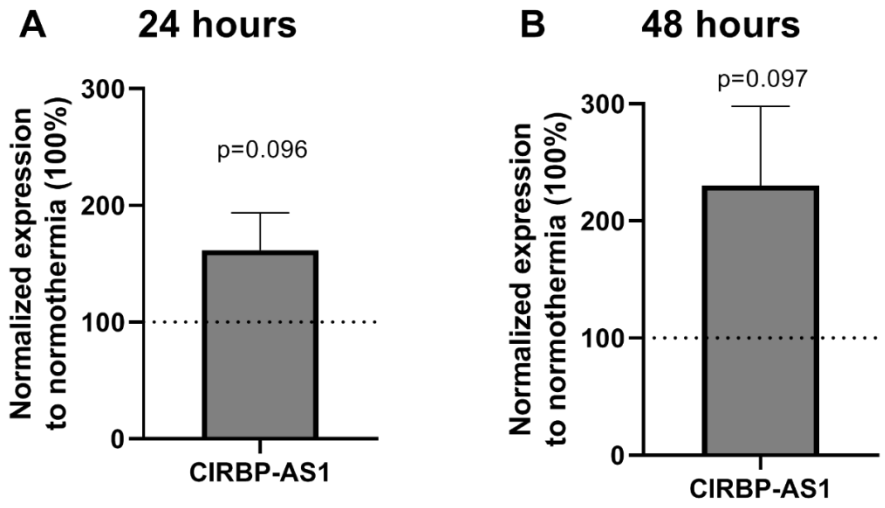

Figure 4A-B CIRBP-AS1 expression under hypothermia in HUVECs. A – CIRBP-AS1 expression after 24 hours of hypothermia showed a trend towards increased expression (p=0.096). B – CIRBP-AS1 expression after 48 hours of hypothermia showed a trend towards increased expression (p=0.097). Mean is indicated relative to GAPDH and normalized to normothermia (dotted line). Error bars represent SEM (N=3). One-sample t-test with a significance level of $\alpha<0.05$ did not show significant changes.

Target microRNAs in hypothermia

As our previous study showed that CIRBP targets 14q32 microRNAs miR-329-3p and miR-495-3p on a post-transcriptional level[18], we determined the levels of all intermediate products of these microRNAs, i.e. primary, precursor and mature microRNA levels. Under hypothermic conditions, no changes in pri-, pre- nor mature microRNA expression of miR-329-3p were observed (Figure 5A-B). Similarly, for miR-495-3p no differences in any stage of microRNA processing was observed (Figure 5C-D).

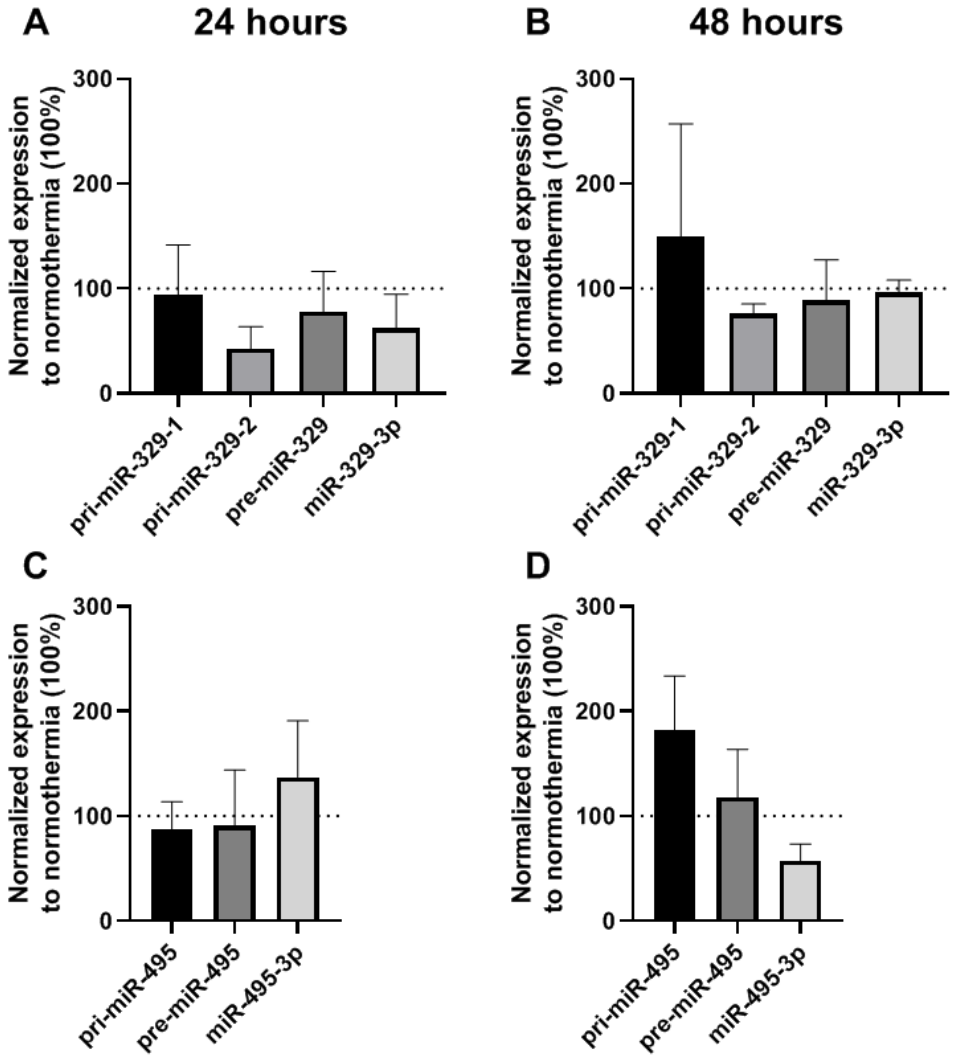

Figure 5A-D 14q32 microRNA expression after 24 or 48 hours hypothermia in HUVECs. A – primary, precursor and mature miR-329-3p expression after 24 hours of hypothermia did not show significant differences compared to normothermia. B – primary, precursor and mature miR-329-3p expression after 48 hours of hypothermia did not show significant differences compared to normothermia. C – primary, precursor and mature miR-495-3p expression after 24 hours of hypothermia did not show significant differences compared to normothermia. D – primary, precursor and mature miR-495-3p expression after 48 hours of hypothermia did not show significant differences compared to normothermia. Mean expression relative to U6 and normalized to normothermic condition (dotted line) is indicated. Error bars represent SEM (N=3). One sample t-test was performed and did not show any significant differences ($\alpha < 0.05$).

CIRBP knockdown with siRNAs

Hypothermic stress induced total CIRBP expression, but it did not affect target microRNA expression. Next, we used an siRNA to silence CIRBP and assessed the expression of total CIRBP and of its splice variants. As shown in Figure 6A, the siRNA was expected to target all splice variants of CIRBP. Total CIRBP expression was indeed knocked down by ~90% (p=0.002). Of the splice variants, especially CIRBP-SV1 was knocked down even further than total CIRBP

(~99% decrease, p=0.002, Figure 6B), whereas other splice variants remained unaffected. When measuring CIRBP-AS1 in CIRBP-silenced cells, we observed a trend towards decreased CIRBP-AS1 expression (40% decrease, p=0.078, Figure 6C).

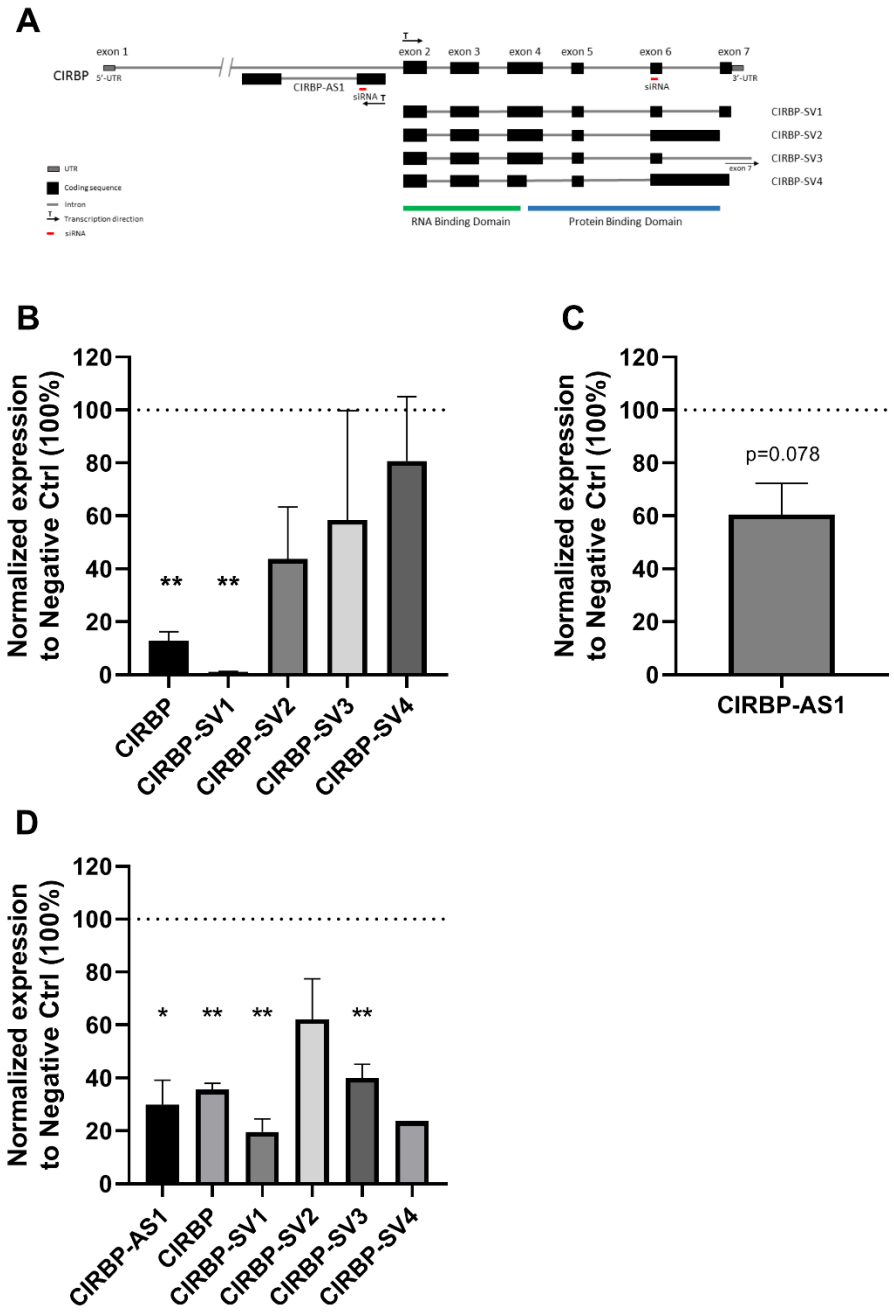

Figure 6A-D CIRBP and CIRBP-AS1 expression after knockdown with siRNAs in HUVECs. A – schematic representation of siRNA target sites along the CIRBP and CIRBP-AS1 genes. B – Expression of total CIRBP and CIRBP splice variants after CIRBP knockdown using siRNA showed a downregulation of total CIRBP by 90% (p=0.002). Of the splice variants, only CIRBP-SV1 showed a knockdown (99%, p=0.002). C – CIRBP-AS1 expression after CIRBP siRNA knockdown showed a trend towards decreased expression (p=0.078). D – CIRBP and CIRBP-AS1 expression after CIRBP-AS1 silencing using siRNA showed effective knockdown of CIRBP-AS1. Total CIRBP was downregulated as well (p=0.017) and of the CIRBP splice variants, only CIRBP-SV1 and CIRBP-SV3 were decreased (p=0.004 and p=0.007 respectively). Mean expression relative to GAPDH is indicated and normalized to negative control siRNA treatment (dotted

line). Error bars represent SEM (N=3). One-sample t-tests were performed with a significance level of $\alpha<0.05$. *$p<0.05$, **$p<0.01$.

CIRBP-AS1 knockdown

After CIRBP knockdown, CIRBP-AS1 changed in a similar direction as total CIRBP, i.e. a ~40% decrease (p=0.078). Next, CIRBP-AS1 was knocked-down using an siRNA (Figure 6A) and expression of CIRBP-AS1, total CIRBP and the CIRBP splice variants was assessed. CIRBP-AS1 knockdown was successful with 70% (p=0.017). In response to CIRBP-AS1 knockdown, total CIRBP was also downregulated by ~65% (p=0.001). When looking at the specific splice variants, CIRBP-SV1 (~80% downregulation, p=0.004) and CIRBP-SV3 (~60% downregulation, p=0.007) were downregulated, whereas the expression of CIRBP-SV2 and CIRBP-SV4 was not affected (Figure 6D).

MicroRNA expression in CIRBP and CIRBP-AS1 knockdown

Then we asked what the effect of CIRBP-silencing was on its target microRNAs. For miR-329-3p no effects on expression levels were observed for either primary and precursor microRNAs or the mature miR-329-3p (Figure 7A). Figure 7B shows that pri-miR-495 and pre-miR-495 also remained unchanged by CIRBP siRNA treatment, compared to Negative Control siRNA. Mature miR-495-3p, however, was affected by CIRBP knockdown and showed a downregulation of ~70% (p=0.02).

Knockdown of CIRBP-AS1 resulted in a ~55% downregulation of mature miR-329-3p (p=0.01), but expression of primary and precursor miR-329 remained unchanged compared to negative control treated HUVECs (Figure 7C). For miR-495-3p, similar results were observed as with siRNA-mediated silencing of CIRBP. Primary and precursor miR-495 expression were not affected, whereas miR-495-3p was significantly downregulated by ~85% (p=0.003) in CIRBP-AS1 knockdown (Figure 7D).

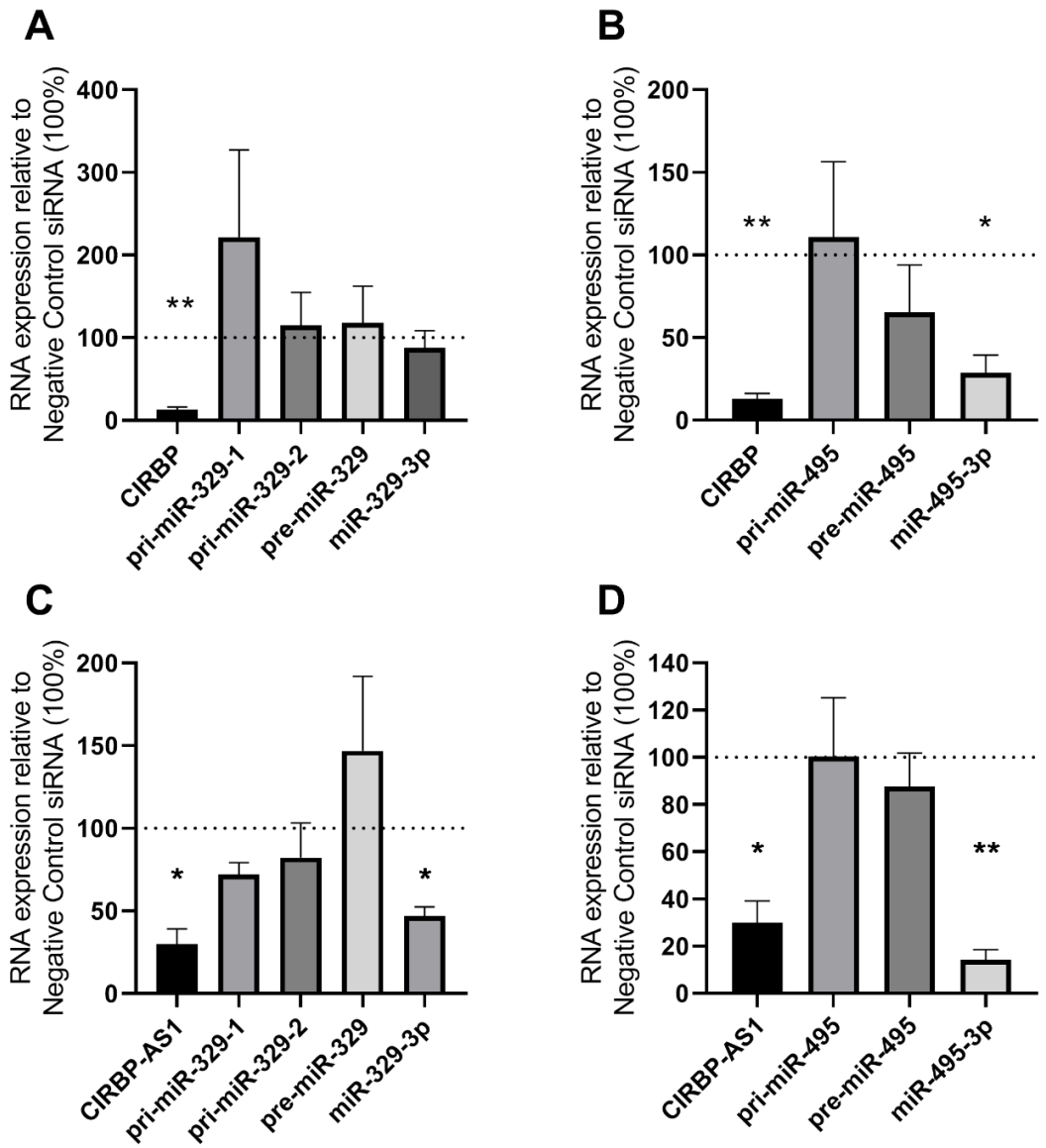

Figure 7A-D MicroRNA expression in HUVECs after CIRBP or CIRBP-AS1 siRNA treatment. A – expression of primary, precursor and mature miR-329-3p after CIRBP knockdown using siRNA did not show differences compared to negative control siRNA treatment. B – expression of primary and precursor miR-495 remained unchanged after knockdown of CIRBP, but mature miR-495-3p was significantly downregulated after CIRBP silencing. C – knockdown of CIRBP-AS1 led to mature miR-329-3p downregulation, but primary and precursor microRNAs remained unchanged. D – expression of primary and precursor miR-495 did not change in CIRBP-AS1 knockdown, but miR-495-3p expression was downregulated. Mean expression relative to U6 (miRs) and GAPDH (CIRBP) is indicated and normalized to negative control siRNA treatment (dotted line). Error bars represent SEM (N=3). One-sample t-tests were performed with a significance level of $\alpha<0.05$. *$p< 0.05$, **$p<0.01$.

Scratch wound healing in HUVECs after CIRBP and CIRBP-AS1 knockdown

Subsequently, the effect on endothelial cell migration as measure of angiogenic potential was assessed, using scratch wound healing assay in siRNA treated endothelial cells. Scratch wound healing in HUVECs after CIRBP knockdown was 4 times higher compared to the negative

control treated cells (p=0.004, Figure 8A+B). Expression of PCNA mRNA in CIRBP knockdown was assessed as a measure of proliferation, but did not show differences compared to negative control treatment (Figure 8C). Furthermore, the angiogenic potential of CIRBP-AS1 knockdown was investigated as well. Knockdown of CIRBP-AS1 resulted in 5-fold increased cell migration compared to negative control treated HUVECs (p=0.0002, Figure 8D+E). PCNA mRNA expression levels were similar in CIRBP-AS1 knockdown and negative control (Figure 8F).

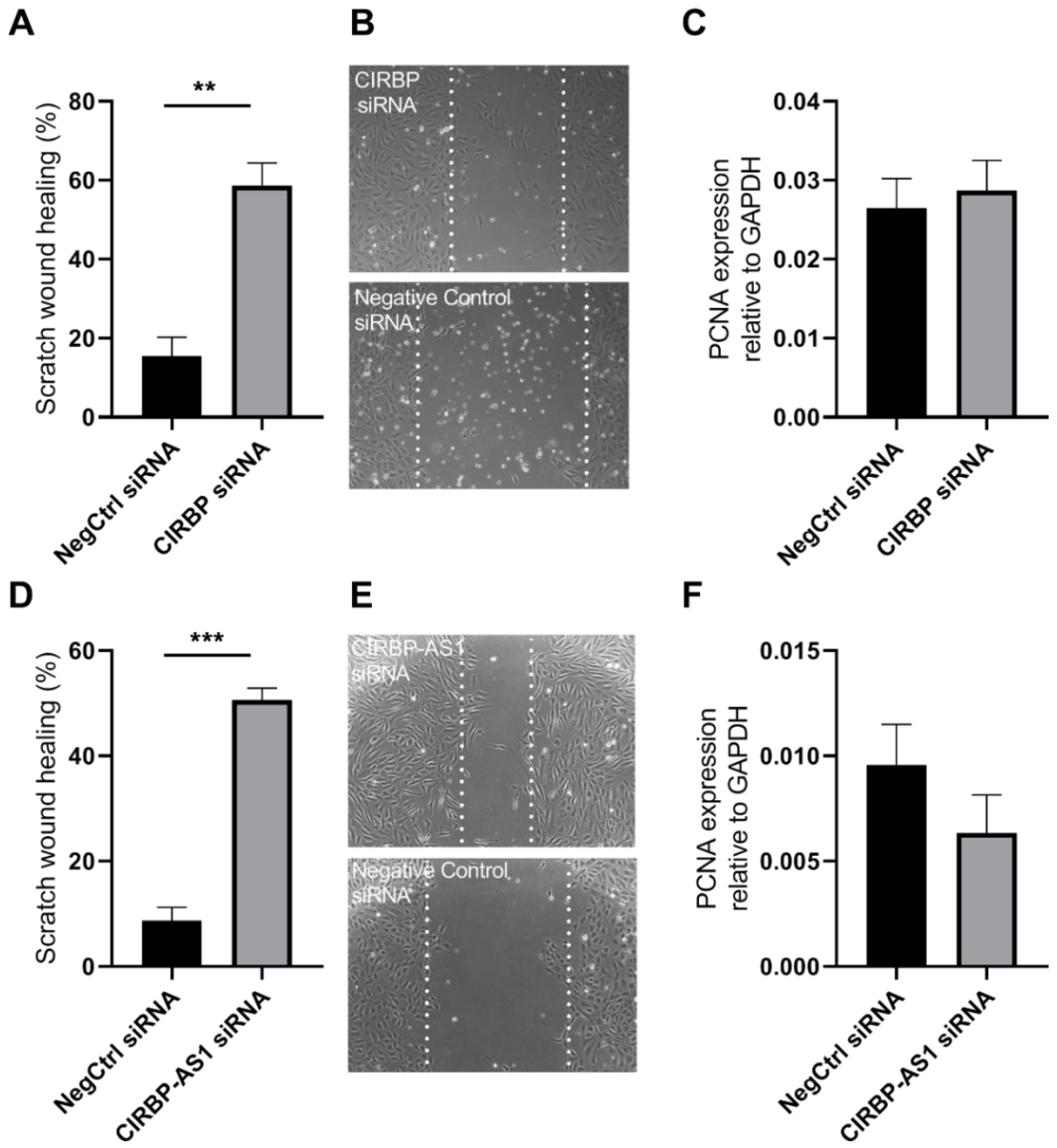

Figure 8A-F Functional assays after CIRBP siRNA treatment in HUVECs. A+B - Scratch wound healing in siRNA CIRBP treatment increased compared to negative control siRNA treatment (p=0.004). C - PCNA expression in HUVECs after CIRBP siRNA treatment did not show differences in expression compared to negative control. D+E – CIRBP-AS1 knockdown resulted in increased cell migration compared to negative control siRNA treated cells (p=0.0002). F - PCNA expression in HUVECs after CIRBP-AS1 siRNA treatment did not show differences in expression compared to negative control. Mean is indicated and error bars represent SEM (N=3). Significant differences were found with independent sample Student's t-test with a significance level of $\alpha<0.05$. **p< 0.01, ***p<0.001.

Tube formation in CIRBP knockdown

Next, we performed Matrigel tube-formation assays with HUVECs treated with siRNAs against CIRBP. As shown in Figure 9, CIRBP siRNA-treated cells showed significantly more segments and branches compared to Negative Control siRNA-treated cells (~100% increase, p=0.046 and ~60% increase p=0.016, respectively). Moreover, the total length of all tubes was increased when CIRBP was knocked down (~25% increase, p=0.014).

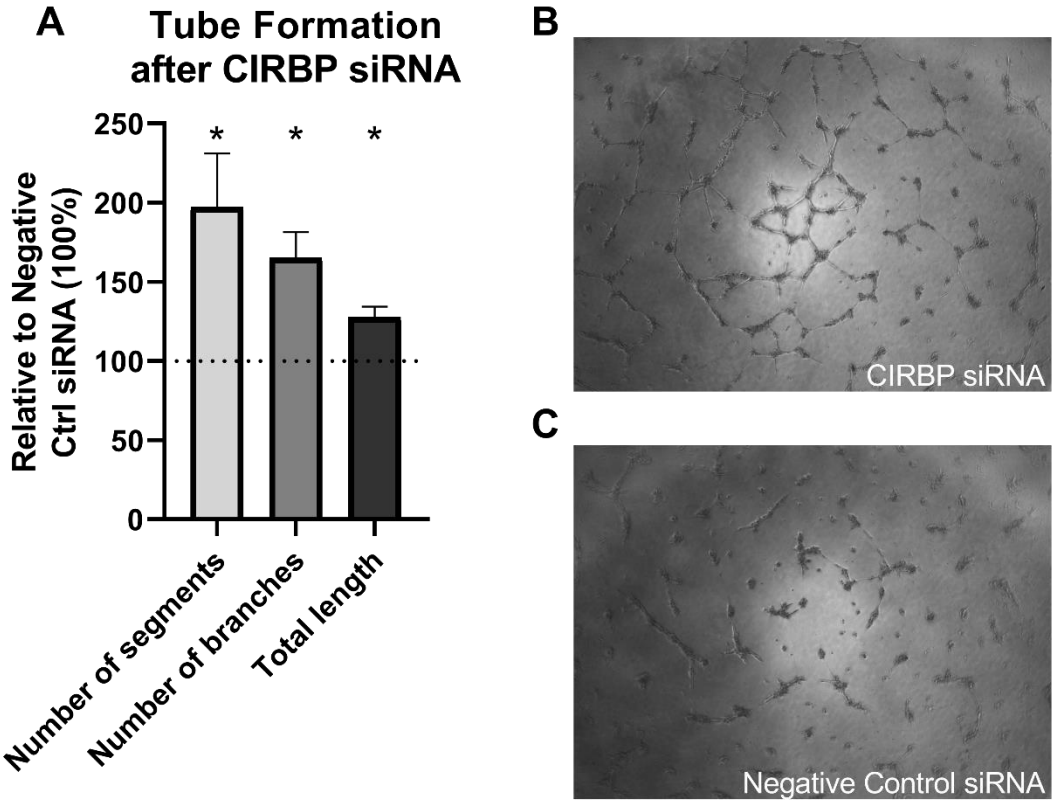

Figure 9A-C Tube formation assay in HUVECs. A – tube formation indicated in number of segments, number of branches and total length of tubes of HUVECs after CIRBP siRNA treatment compared to Negative Control siRNA treatment. Mean is indicated and error bars represent SEM (N=5). Indicated bars show significant change to Negative Control siRNA treated HUVECs (dotted line), found with one-sample t-test. *p< 0.05 with a significance level of $\alpha<0.05$. B+C – pictures of siRNA treated HUVECs at 12 hours after start of tube formation in CIRBP siRNA-treaded and negative control siRNA treated cells, respectively.

Discussion

In this study, we investigated Cold-Inducible RNA Binding Protein (CIRBP) as a potential therapeutic target to stimulate angiogenesis in patients with PAD. We show that CIRBP is upregulated under hypothermic conditions and, when we directly inhibit CIRBP expression, cell migration and tube formation capacity of endothelial cells is promoted. Upon inhibition of CIRBP, miR-495-3p expression is downregulated as well, suggesting that pro-angiogenic properties of CIRBP may act via miR-495.

We confirm that CIRBP is regulated under hypothermic conditions, as was reported previously[1, 3-6]. The novelty of this study, however, is that we showed this in vascular endothelial cells that were subjected to hypothermic conditions, as frequently occurs in PAD. CIRBP has four splice variants that alter the coding sequence. Of these four variants, CIRBP-SV1 specifically showed a trend towards upregulation after 24 and 48 hours of hypothermia. When we knocked-down CIRBP using an siRNA, we again observed specific knockdown of CIRBP-SV1 (as well as of total CIRBP). This was unexpected, as the binding site of the siRNA was predicted to target an mRNA sequence that is present in all four splice variants.

The antisense strand of CIRBP encodes a long noncoding RNA, CIRBP-AS1, of which the function has not yet been elucidated. We observed a trend towards upregulation of CIRBP-AS1 under hypothermic conditions, although the response to hypothermia was slower than that of CIRBP itself. After CIRBP knockdown, CIRBP-AS1 expression decreased and the opposite was also true. Inhibition of CIRBP-AS1 with an siRNA resulted in simultaneous downregulation of total CIRBP and of CIRBP-SV1 and CIRBP-SV3 expression. Potentially, a positive feedback loop supports transcription of the CIRBP locus, where CIRBP and CIRBP-AS1 induce each other's expression.

The expression of 14q32 microRNAs miR-329-3p and miR-495-3p was not increased under hypothermia, even though the expression of their reported post-transcriptional regulator CIRBP was increased. In contrast, silencing of CIRBP using an siRNA did lead to a decrease in miR-495-3p expression. Likely, the processing rate of 14q32 microRNAs is already at an optimum under normothermic conditions, which explains that an increase in CIRBP does not induce more processing of precursor microRNAs. The dramatic decrease in CIRBP expression does result in insufficient processing of miR-495-3p however. Surprisingly though, expression of miR-329-3p was still unaffected. Furthermore, CIRBP-AS1 knockdown resulted in a decreased expression of both mature microRNAs. However, regulation of microRNA

expression is highly complex and involves many RBPs that may compensate for the loss of CIRBP. Processing of miR-329-3p, but not miR-495-3p, for example, is also enhances by the RBP Myocyte Enhancer Factor 2A (MEF2A)[17]. When we speculate what these findings could mean to human PAD, CIRBP expression would likely be increased, as patients suffer from cold extremities. However, induced CIRPB does not affect 14q32 microRNA expression and thus, there would likely be only minor effects on angiogenesis. Therapeutic silencing of CIRBP however, would decrease the expression of mature miR-495-3p, which has profound effects on ischemia-induced neovascularization and thus on perfusion of the affected limb[20].

Therefore, we assessed these potential pro-angiogenic features of CIRBP knockdown. Indeed, both cell migration assays and tube formation assays in HUVECs showed an increase in angiogenic potential following CIRBP and CIRBP-AS1 knockdown. We know that direct inhibition of miR-495-3p promotes angiogenesis[20] and we observed here that CIRBP knockdown leads to decreased expression of miR-495-3p. These findings of course suggest that the increased angiogenic potential induced by CIRBP downregulation is accomplished via the subsequent miR-495-3p decrease. However, it remains to be determined whether CIRBP can also target additional pro-angiogenic factors.

It has been shown in CIRBP$^{-/-}$ mice that the inflammatory response in tissue wound healing is faster than in wildtype mice. More CD31 expression, as marker of endothelial cells and thus angiogenesis, was observed in wounds of CIRBP$^{-/-}$ mice[25], although the exact mechanism of action for CIRBP in wound healing was not elucidated. The inflammatory function of CIRBP in stress conditions was already reported by Qiang et al[26]. Moreover, the authors reported that CIRBP binds TLR4, MD2 and the TLR4/MD2-complex, which is known to stimulate neovascularization. Therefore, the question arises whether CIRBP binding to TLR4 increases or decreases TLR4 availability. If the latter is the case, CIRBP-silencing would increase TLR4 availability and this may therefore be an explanation for increased neovascularization after CIRBP inhibition.

We found that inhibition of CIRBP leads mainly to a decrease in CIRBP-SV1, which then resulted in increased *in vitro* angiogenesis. It would be interesting in future research to target CIRBP-SV2-4 specifically and assess the effect on angiogenesis, and on 14q32 microRNA expression, for these splice variants separately. With this, we could better understand the exact part of the CIRBP sequence that targets microRNA expression and, possibly, link this to the pro-angiogenic potential of CIRBP. Since the RNA binding domain is similar in all splice variants, it is likely that all bind to precursor microRNAs in a similar manner. However, the

splice variants differ in their protein binding domains, which could result in the attraction of different proteins. This may still lead to changes in microRNA processing, but may also influence angiogenesis more directly via these proteins.
Silencing of CIRBP-AS1, like of CIRBP, resulted in increased angiogenesis and decreased mature microRNA expression. Furthermore, downregulation of CIRBP-AS1 decreased CIRBP expression and vice versa. However, we did not yet uncover whether CIRBP or CIRBP-AS1 is the key regulating factor in angiogenesis and thus the main potential therapeutic target in stimulating neovascularization. Moreover, as both CIRBP and CIRBP-AS1 are able to downregulate expression of mature 14q32 microRNAs, it remains to be determined whether CIRBP-AS1 can affect microRNA processing directly and, thereby, play a role in angiogenesis.

We found that hypothermia caused CIRBP expression upregulation and that CIRBP silencing resulted in proangiogenic features. Therefore, one could speculate that hyperthermia leads to decreased CIRBP expression, followed by subsequent increase in angiogenesis. In PAD, this would imply that warming affected cold legs could lead to increased angiogenesis and therefore to improved circulation. A next step in this study could be to assess whether increased temperature causes decreased CIRBP expression in endothelial cells and subsequent miR-495-3p downregulation.

In conclusion, our findings demonstrate that hypothermia induces CIRBP expression, but does not affect 14q32 microRNAs miR-329-3p and miR-495-3p expression. Silencing of CIRBP decreases miR-495-3p expression and promotes *in vitro* angiogenesis. CIRBP-AS1 is affected by CIRBP knockdown and silencing of CIRBP-AS1 also inhibits CIRBP expression. Furthermore CIRBP-AS1 knockdown inhibits both miR-329-3p and miR-495-3p and promotes *in vitro* angiogenesis as well. This makes CIRBP and CIRBP-AS1 promising targets in post-ischemic neovascularization. Future studies will determine whether these targets work in an *in vivo* model as well.

References

1. Liu A, Zhang Z, Li A, Xue J. Effects of hypothermia and cerebral ischemia on cold-inducible RNA-binding protein mRNA expression in rat brain. Brain research 2010;1347:104-110.
2. Wellmann S, Buhrer C, Moderegger E, Zelmer A, Kirschner R, Koehne P, Fujita J, Seeger K. Oxygen-regulated expression of the RNA-binding proteins RBM3 and CIRP by a HIF-1-independent mechanism. Journal of cell science 2004;117:1785-1794.
3. Liao Y, Tong L, Tang L, Wu S. The role of cold-inducible RNA binding protein in cell stress response. International journal of cancer 2017;141:2164-2173.
4. Al-Fageeh MB, Smales CM. Cold-inducible RNA binding protein (CIRP) expression is modulated by alternative mRNAs. RNA (New York, NY) 2009;15:1164-1176.
5. Lleonart ME. A new generation of proto-oncogenes: cold-inducible RNA binding proteins. Biochimica et biophysica acta 2010;1805:43-52.
6. Fujita J. Cold shock response in mammalian cells. Journal of molecular microbiology and biotechnology 1999;1:243-255.
7. Nishiyama H, Itoh K, Kaneko Y, Kishishita M, Yoshida O, Fujita J. A glycine-rich RNA-binding protein mediating cold-inducible suppression of mammalian cell growth. The Journal of cell biology 1997;137:899-908.
8. Nishiyama H, Higashitsuji H, Yokoi H, Itoh K, Danno S, Matsuda T, Fujita J. Cloning and characterization of human CIRP (cold-inducible RNA-binding protein) cDNA and chromosomal assignment of the gene. Gene 1997;204:115-120.
9. Zhu X, Buhrer C, Wellmann S. Cold-inducible proteins CIRP and RBM3, a unique couple with activities far beyond the cold. Cellular and molecular life sciences : CMLS 2016;73:3839-3859.
10. Zhong P, Huang H. Recent progress in the research of cold-inducible RNA-binding protein. Future science OA 2017;3:Fso246.
11. Horii Y, Shiina T, Uehara S, Nomura K, Shimaoka H, Horii K, Shimizu Y. Hypothermia induces changes in the alternative splicing pattern of cold-inducible RNA-binding protein transcripts in a non-hibernator, the mouse. Biomedical research (Tokyo, Japan) 2019;40:153-161.
12. Pelechano V, Steinmetz LM. Gene regulation by antisense transcription. Nature reviews Genetics 2013;14:880-893.
13. Gomes CP, Nobrega-Pereira S, Domingues-Silva B, Rebelo K, Alves-Vale C, Marinho SP, Carvalho T, Dias S, Bernardes de Jesus B. An antisense transcript mediates MALAT1 response in human breast cancer. BMC cancer 2019;19:771.
14. Zong X, Nakagawa S, Freier SM, Fei J, Ha T, Prasanth SG, Prasanth KV. Natural antisense RNA promotes 3' end processing and maturation of MALAT1 lncRNA. Nucleic Acids Res 2016;44:2898-2908.
15. Bernstein E, Caudy AA, Hammond SM, Hannon GJ. Role for a bidentate ribonuclease in the initiation step of RNA interference. Nature 2001;409:363-366.
16. Lee Y, Jeon K, Lee JT, Kim S, Kim VN. MicroRNA maturation: stepwise processing and subcellular localization. Embo j 2002;21:4663-4670.
17. Welten SMJ, de Vries MR, Peters EAB, Agrawal S, Quax PHA, Nossent AY. Inhibition of Mef2a Enhances Neovascularization via Post-transcriptional Regulation of 14q32 MicroRNAs miR-329 and miR-494. Molecular therapy Nucleic acids 2017;7:61-70.
18. Downie Ruiz Velasco A, Welten SMJ, Goossens EAC, Quax PHA, Rappsilber J, Michlewski G, Nossent AY. Posttranscriptional Regulation of 14q32 MicroRNAs by the CIRBP and HADHB during Vascular Regeneration after Ischemia. Molecular therapy Nucleic acids 2019;14:329-338.
19. Treiber T, Treiber N, Plessmann U, Harlander S, Daiss JL, Eichner N, Lehmann G, Schall K, Urlaub H, Meister G. A Compendium of RNA-Binding Proteins that Regulate MicroRNA Biogenesis. Molecular cell 2017;66:270-284.e213.

20. Welten SM, Bastiaansen AJ, de Jong RC, de Vries MR, Peters EA, Boonstra MC, Sheikh SP, Monica NL, Kandimalla ER, Quax PH, Nossent AY. Inhibition of 14q32 MicroRNAs miR-329, miR-487b, miR-494, and miR-495 increases neovascularization and blood flow recovery after ischemia. Circ Res 2014;115:696-708.
21. Welten SMJ, de Jong RCM, Wezel A, de Vries MR, Boonstra MC, Parma L, Jukema JW, van der Sluis TC, Arens R, Bot I, Agrawal S, Quax PHA, Nossent AY. Inhibition of 14q32 microRNA miR-495 reduces lesion formation, intimal hyperplasia and plasma cholesterol levels in experimental restenosis. Atherosclerosis 2017;261:26-36.
22. Wezel A, Welten SM, Razawy W, Lagraauw HM, de Vries MR, Goossens EA, Boonstra MC, Hamming JF, Kandimalla ER, Kuiper J, Quax PH, Nossent AY, Bot I. Inhibition of MicroRNA-494 Reduces Carotid Artery Atherosclerotic Lesion Development and Increases Plaque Stability. Annals of surgery 2015;262:841-847; discussion 847-848.
23. Welten SM, Goossens EA, Quax PH, Nossent AY. The multifactorial nature of microRNAs in vascular remodelling. Cardiovascular research 2016;110:6-22.
24. Risau W. Mechanisms of angiogenesis. Nature 1997;386:671-674.
25. Idrovo JP, Jacob A, Yang WL, Wang Z, Yen HT, Nicastro J, Coppa GF, Wang P. A deficiency in cold-inducible RNA-binding protein accelerates the inflammation phase and improves wound healing. International journal of molecular medicine 2016;37:423-428.
26. Qiang X, Yang WL, Wu R, Zhou M, Jacob A, Dong W, Kuncewitch M, Ji Y, Yang H, Wang H, Fujita J, Nicastro J, Coppa GF, Tracey KJ, Wang P. Cold-inducible RNA-binding protein (CIRP) triggers inflammatory responses in hemorrhagic shock and sepsis. Nature medicine 2013;19:1489-1495.

Supplementary Data

Supplementary Table 1 sequences of primers used for qPCR and of siRNAs used for knockdown

	Forward sequence	Reverse sequence
HSA-CIRBP	TTGACACCAATGAGCAGTCG	GGCATCCTTAGCGTCGTCAA
HSA-splice variant 1	CGTGGGTTCTCTAGAGGAGGA	CTCGTTGTGTGTAGCGTAACTG
HSA-splice variant 2	CGTGGGTTCTCTAGAGGAGGA	CGCCCTCGGAGTGTGACTTA
HSA-splice variant 3	CGTGGGTTCTCTAGAGGAGGA	TCAACCGTAACTGTCATAACTG
HSA-splice variant 4	GTAGACCAGGCAGGAGGAG	CGCCCTCGGAGTGTGACTTA
HSA-CIRBP-AS1	CAATGGGAAAAGGAGGAAACT	CCTTGTAAAGCTGGTTCTCCA
GAPDH	CACCACCATGGAGAAGGC	AGCAGTTGGTGGTGCAGGA
HSA-pri-miR-329-1	TGGGGAAGAATCAGTGGTGT	GACCAGAAGGCCTCCAAGAT
HSA-pri-miR-329-2	TGTCAAGTTTGGGGAAGGAA	GACCAGAAGGCCTCCAAGAT
HSA-pre-miR-329	TGAAGAGAGGTTTTCTGGGTTT	ACCAGGTGTGTTTCGTCCTC
HSA-pri-miR-495	CTGACCCTCAGTGTCCCTTC	ATGGAGGCACTTCAAGGAGA
HSA-pre-miR-495	GCCCATGTTATTTTCGCTTT	CCGAAAAAGAAGTGCACCAT
U6	AGAAGATTAGCATGGCCCCT	ATTTGCGTGTCATCCTTGCG
siRNA CIRPB	GAGUCAGAGUGGUGGCUAC	
siRNA CIRBP-AS1	CAGGACCCUCACUCACUA	